論文内容の要旨

論文題目： Fabrication and magnetic properties of Co metal nanoparticles embedded in a transparent oxide matrix
（透明酸化物中に内包させた Co 金属ナノ粒子の作製と磁気特性）

氏名： 池宮桂

Introduction

The objective of this work is to prepare ferromagnetic 3*d* metal nanoparticles and investigate their magnetic properties, especially ultrafast demagnetization dynamics.

Ultrafast demagnetization has been observed in many systems; however, most of the observations have been made in bulk or thin films and few have been reported on ferromagnetic 3*d* metal nanoparticles. Metal nanoparticles are easily oxidized in ambient atmospheres, resulting in deterioration of the ferromagnetic properties. This instability makes the observation in metal nanoparticles difficult. Ferromagnetic metal nanoparticles have shape- or size-dependent magnetism. Fabrication of stable metal nanoparticles is, therefore, required for better understanding of ferromagnetism.

In this work, I propose a novel method for fabricating Co nanorods with various size and Ag-Co matchsticks, both of which are embedded in an anatase TiO_2 matrix, thereby being stabilized. These Co nanostructures are prepared utilizing self-assembly process by pulsed laser deposition (PLD).

Ag-Co matchsticks were prepared in order to investigate the effect of localized surface plasmon resonance (LSPR) on demagnetization process. Remarkably enough, Ag-Co nanomatchsticks grew nearly in parallel to the film normal. These oriented Ag-Co nanomatchsticks are advantageous when LSPR of different modes are studied. Although there are many reports on such hybrid matchstick-like structures, most of the structures were fabricated by solution-growth technique, so that they were randomly oriented.

Finally, time-resolved Faraday effect measurements were performed on these Co nanorods and Ag-Co nanomatchsticks to observe ultrafast demagnetization. Enhanced demagnetization was observed in Ag-Co nanomatchsticks. This enhanced demagnetization is probably due to LSPR of Ag.

Experimental

Epitaxial thin films of (001)-oriented anatase TiO_2 containing Co nanorods (Co:TiO_2) and those containing Ag-Co nanomatches (Ag_x,Co:TiO_2) were prepared on $LaSrAlO_4$ (LSAO) (001) single-crystalline substrates by pulsed laser deposition (PLD). A Kr-F excimer laser (wavelength = 248 nm) operated with a laser fluence of 2 J cm^{-2} $pulse^{-1}$ and a repetition rate of 2 Hz was used for ablation.

To obtain the crystallized anatase TiO_2 phase in a relatively low temperature range, I used a seed-layer of pure TiO_2, as described below. Sintered pellets of pure TiO_2 ,a mixture of TiO_2 and CoO (molar ratio Ti:Co = 95:5),

and a mixture of TiO_2, CoO, and Ag_2O (molar ratio Ti:Co:Ag = 95:5:x) were used as target materials for the anatase TiO_2 seed layers, Co:TiO_2 films, and Ag_x,Co:TiO_2 films, respectively.
The crystallinity and crystallographic orientation of the obtained films were evaluated by X-ray diffraction (XRD). The surface topography was characterized by atomic force microscopy (AFM). The sizes and distribution of the Co nanorods were examined by transmission electron microscopy (TEM) with the aid of energy dispersive X-ray analysis (TEM-EDX), scanning TEM (STEM), and high-angle annular dark field STEM (HAADF-STEM). The crystal structure of the Co nanorods was determined from nanobeam electron diffraction patterns. Magnetic properties were measured by a superconducting quantum interference device (SQUID) magnetometer (MPMS XL; Quantum Design, San Diego, CA, USA) and a UV–vis magneto-optical spectrometer (BH-M800UV-KC-KF; Neoark Corp., Tokyo, Japan). To measure ultrafast demagnetization dynamics, time-resolved Faraday effect measurement using pump-probe technique was performed for these films. A Ti:sapphire laser operating at 100 kHz was used. The fundamental wavelength was 800 nm and the pulse duration was 220 fs. The wavelength of probe pulses was set to 800 nm and that of pump pulses, which were generated by frequency doubling, was 400 nm. An external magnetic field of 9 kOe was applied perpendicular to the film surfaces. All measurements were performed at room temperature.

Preparation of Co:TiO_2 nanocomposite films

It was found that the Co:TiO_2 films directly deposited on LSAO substrate do not show good crystallinity particularly at low temperatures. To obtain high-crystallinity anatase TiO_2 phase over a wider temperature range, I used a seed-layer of pure TiO_2, as follows.

An anatase TiO_2 seed layer was first deposited on an LSAO substrate at T_s = 650 °C and P_{O2} = 5 × 10^{-3} Torr, and then a Co:TiO_2 thin film was grown at different substrate temperatures in the range T_s = 200-400 °C and at an oxygen pressure P_{O2} = 1.0 × 10^{-6} Torr. The thicknesses of the TiO_2 seed layer and the Co:TiO_2 film were set at 5 nm and 28 nm, respectively.

According to magnetization measurement, Co concentrations in Co:TiO_2 are estimated to be 4.3%, 3.7%, and 3.3% for T_s = 250 °C, 300 °C, and 350 °C, respectively. These values are close to the Co content of the Co:TiO_2 target (5%), implying that in these films Co exists mostly as nanoparticles of fcc Co metal, that is, the Co nanoparticles do not undergo oxidation even though they are embedded in the oxide matrix.

In the films grown at T_s = 200 °C and 400 °C, the calculated fcc-Co contents are as low as ~0.7%. At T_s = 400 °C, it is likely that Co reacts with O or Ti to form nonmagnetic oxides such as CoO and $CoTiO_3$, resulting in the decrease in magnetization.

TEM results for the Co:TiO_2/TiO_2 films grown at T_s = 250 °C, 300 °C, and 350 °C are summarized in figure 1. Plane-view and cross-sectional TEM images in figures 1(a)–(c) exhibit well-defined cylindrical nanostructures with long-axes nearly perpendicular to the film planes. The nanostructures are imaged with brighter contrast, suggesting that they are rich in a heavier element, Co. Nanobeam electron diffraction measurements at the Co rich regions revealed that they are Co single crystals with an fcc structure. These results clearly indicate that fcc Co nanorods are embedded in the TiO_2 matrix.

The average diameter and height of the Co nanorods estimated from the TEM images are 9 nm and 10 nm, 10 nm and 22 nm, and 16 nm and 17 nm for the films grown at T_s = 250 °C, 300 °C, and 350 °C, respectively, yielding the average volume of individual Co nanorods as 640 nm^3,

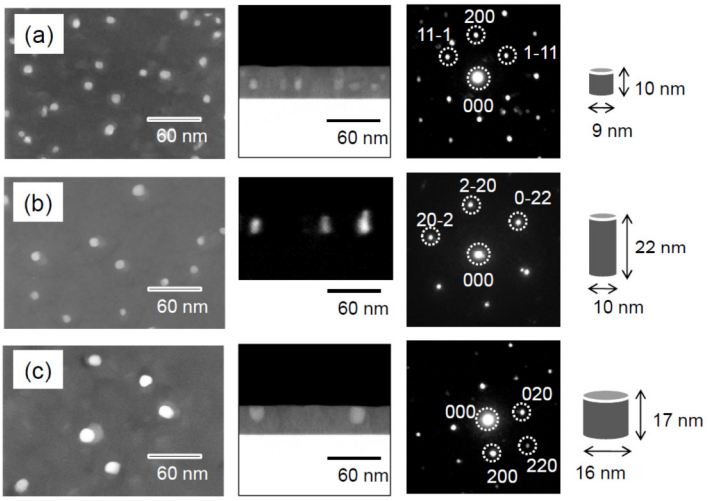

Figure 1 Planar and Cross-sectional TEM images, nanobeam electron diffraction patterns, and the shapes of each Co nanoparticles of Co:TiO_2/TiO_2 films (from left to right) prepared at T_s = (a) 250 °C, (b) 300 °C, and (c) 350 °C.

1700 nm^3, and 3400 nm^3, respectively. The systematic increase of the average volume with increasing T_s is consistent with a kinetic picture that Co atoms become more mobile at higher temperatures.

In this nanocomposite fabrication technique, it is essential to use an anatase TiO_2 seed layer, which lowers the crystallization temperature of anatase TiO_2. In a T_s region of 250 - 350 °C, both high crystallinity of anatase TiO_2 matrix and moderate condensation of Co clusters cab be realized at the same time. In this T_s region, furthermore, the shape and size of fcc-Co nanoparticles embedded in anatase TiO_2 matrix is controllable by T_s.

Preparation of AgCo:TiO_2 nanocomposite films

The anatase TiO_2 seed layers were prepared in the same manner as that for Co:TiO_2. Then a Ag_x,Co:TiO_2 thin film was grown at a substrate temperature T_s = 300 °C and at an oxygen pressure P_{O2} = 1.0 $\times 10^{-6}$ Torr. The thicknesses of the anatase TiO_2 seed layer and the Ag_x,Co:TiO_2 film were set to 5 nm and 30 nm, 5 nm and 38 nm, and 6 nm and 36 nm for x = 5, 10, 20, respectively.

XRD measurements confirmed the anatase TiO_2 phase with (001) orientation for all x.

TEM results for the Ag_{20}Co:TiO_2 films are shown in Fig. 2. A plane-view STEM-EDX image in Fig. 2 exhibits Co nanoparticles with an almost regular size embedded in the TiO_2 matrix. The average diameter of the Co nanoparticles is 5 nm. The molar ratio of Ti:Co:Ag is calculated to be 95:3.6:14 using the image. From magnetization measurements, the Co molar ratio is estimated to be r_{Ti} : R_{Co} = 95:3.9. These values are close to that of the Ag_{20},Co:TiO_2 target (95:5:20). This indicates that in the present Ag_x,Co:TiO_2/TiO_2 films, Co exists mostly as nanoparticles of fcc-Co metal.

When Ag was co-doped into Co:TiO_2 films, interestingly, Ag and Co atoms were completely separated in the film-growing direction and characteristic Ag-Co "nano-matchstick" structures, each of which consists of Co match head and Ag matchstick, were formed in the films, though Ag and Co atoms were deposited simultaneously.

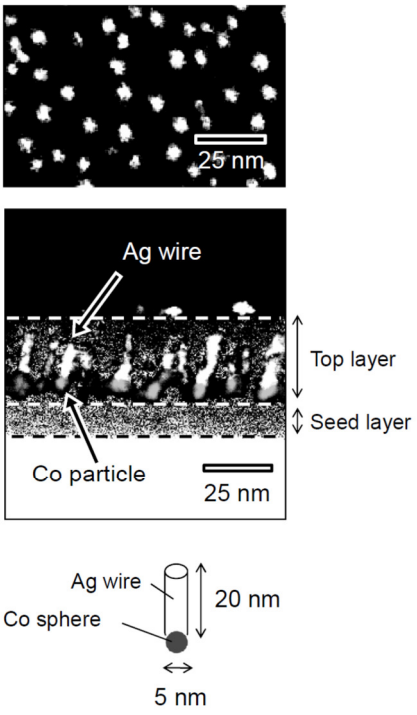

Figure 2 STEM-EDX images of Ag_{20}Co:TiO_2 film. A planar image of Co K (White) (top) and a cross-sectional image of Co K (Gray) and Ag L (White) (middle), and a structure consists of a Co sphere and an Ag wire (bottom).

Magneto-optical property

Faraday ellipticity spectra and absorption spectra of the films are depicted in figure 3(a) and (b). The Faraday ellipticity spectra of the Co:TiO_2/TiO_2 films and the Ag_xCo:TiO_2/TiO_2 films have a similar shape. In the absorption spectra, however, absorption peaks around 450 nm resulting from Ag LSPR are found in Ag_xCo:TiO_2/TiO_2 films and the intensity of the peaks increases with increasing x.

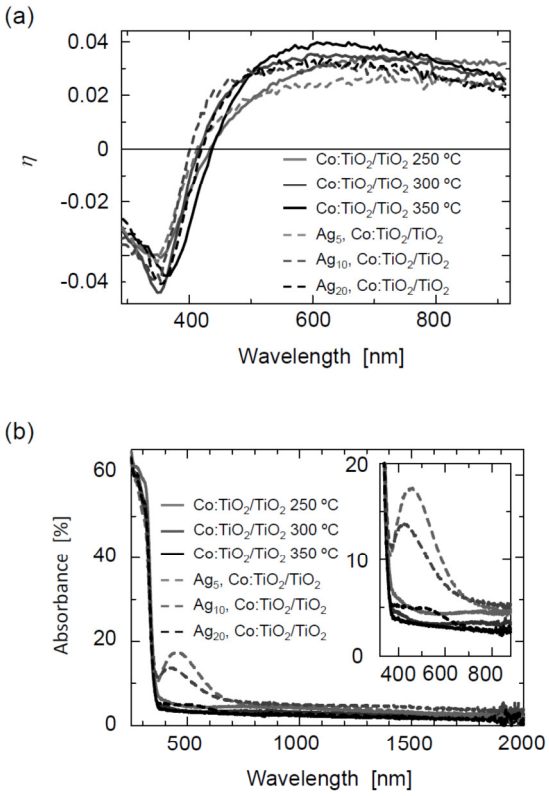

Figure 3 (a) Faraday ellipticity spectra and (b) absorption spectraof Co:TiO_2 films and Ag_xCo:TiO_2 films.

Magnetization dynamics induced by optical pulses

Time-resolved Faraday measurements were performed on the Co:TiO_2/TiO_2 films and the Ag_xCo:TiO_2/TiO_2 films. Figure 4 shows normalized time-dependent differential Faraday ellipticity ($\Delta\eta/\eta$, η denotes saturation values of

Faraday ellipticity in Figure 3(a)) of these films measured under pump fluency of 0.06 mJ cm^{-2}. Ultrafast demagnetization was observed. The amplitudes of the demagnetization (maximum value of the $-\Delta\eta/\eta$) are plotted in figure 5.

As shown in Figure 5(a), The amplitude of the $Co:TiO_2/TiO_2$ films (T_s = 250, 300, and 350 ºC) and the $Ag_5Co:TiO_2/TiO_2$ film exhibit similar $\Delta\eta/\eta$. For the $Ag_xCo:TiO_2/TiO_2$ (x = 5, 10, 20) films, however, the amplitude of $\Delta\eta/\eta$ increases with increasing x. (Figure 5(b))

The possible reasons for this are as follows: 1) different shape of the Co nanoparticles in the films; and 2) different Ag content in the films.

The $Co:TiO_2/TiO_2$ films (T_s = 250, 300, and 350 ºC) and the $Ag_5Co:TiO_2/TiO_2$ film contain Co nanoparticles in different sizes. Especially, the $Ag_5Co:TiO_2/TiO_2$ film contains much smaller Co nanosperes whose size is nearly within the superparamagnetic limit. However, the $\Delta\eta/\eta$ values of the $Co:TiO_2/TiO_2$ films (T_s = 250, 300, and 350 ºC) and the $Ag_5Co:TiO_2/TiO_2$ film exhibit similar behavior. This means that the shape of Co nanoparticles does not affect $\Delta\eta/\eta$ so much.

Therefore, the difference in $\Delta\eta/\eta$ is considered to be caused by difference in Ag content. As shown in figure 3(b), the intensity of Ag LSPR at wavelength of 400 nm increases with increasing x. The Co nanoparticles absorb energy of pump pulses with wavelength of 400 nm efficiently through the Ag LSPR. This results in enhanced demagnetization in the $Ag_xCo:TiO_2/TiO_2$ (x = 10, 20) films. As shown in figure 3(b), the $Ag_5Co:TiO_2/TiO_2$ film shows only small absorbance, compared to the $Co:TiO_2/TiO_2$ films (T_s = 250, 300, and 350 ºC), at wavelength of 400 nm. Accordingly, the magnitude of the demagnetization in the $Ag_5Co:TiO_2/TiO_2$ film is as small as that in the $Co:TiO_2/TiO_2$ films (T_s = 250, 300, and 350 ºC).

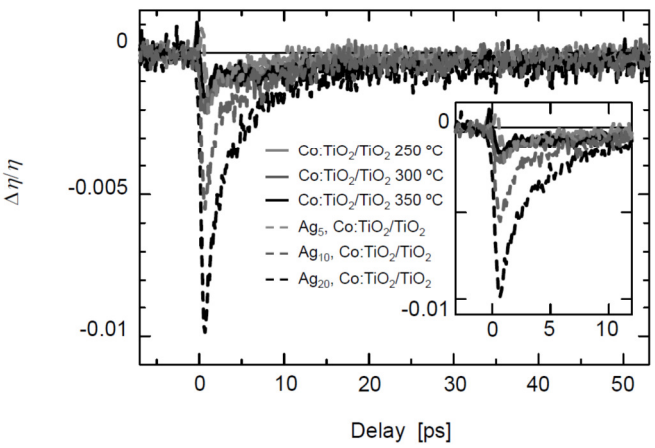

Figure 4 Magnetization dynamics of the $Co:TiO_2$ (300 ºC) film and the $Ag_{20}Co:TiO_2$.

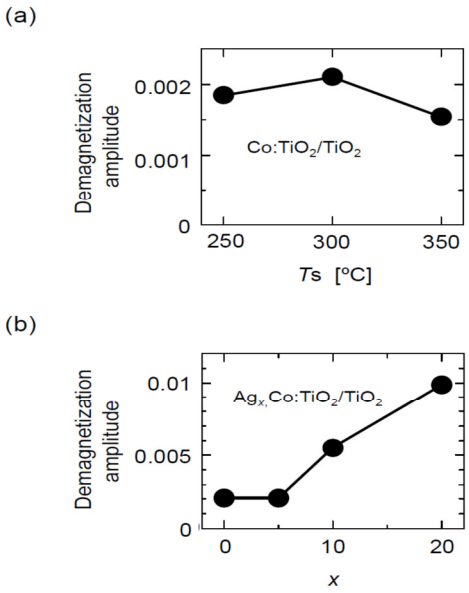

Figure 5 Demagnetization amplitudes of (a) $Co:TiO_2/TiO_2$ films and (b) $Ag_x,Co:TiO_2/TiO_2$ films

Summary

Nanocomposite thin films consisting of an anatase TiO_2 matrix with fcc-Co nanorods ($Co:TiO_2/TiO_2$ film) and those of an anatase TiO_2 matrix with Ag-Co nanomatches ($Ag_x,Co:TiO_2/TiO_2$ film) were successfully prepared. These films were prepared using self-assembly by pulsed laser deposition (PLD). The size of Co nanorods in $Co:TiO_2/TiO_2$ film is controlled by growth temperature. The Ag-Co nanomatches in $Ag_x,Co:TiO_2/TiO_2$ films were oriented and show localized surface plasmon resonance (LSPR) of Ag. The intensity of LSPR increases with increasing Ag content x. Ti has larger oxygen affinity than that of Co, therefore, an anatase TiO_2 matrix protects Co nanoparticles from oxidation and chemically stable.

Time-resolved Faraday effect measurements were performed on these Co nanorods and Ag-Co nanomatchsticks to observe ultrafast demagnetization. Differential Faraday ellipticity values ($\Delta\eta/\eta$) of the $Co:TiO_2/TiO_2$ films and the $Ag_xCo:TiO_2$ (x = 5) film exhibit similar behavior. This means that the shape of Co nanoparticles does not affect $\Delta\eta/\eta$ so much. However, enhanced demagnetization amplitude was found in the $Ag_xCo:TiO_2/TiO_2$ (x = 10, 20) films. This phenomenon can be understood by ultrafast energy transfer from Ag LSPR to electron system or spin system of the $Ag_xCo:TiO_2/TiO_2$ films. The investigation also showed that demagnetization recovery process of the $Ag_xCo:TiO_2/TiO_2$ films depends on Ag content x.